SUPPLEMENTARY INFORMATION

Adhesive Loose Packing of Small Dry Particles

Wenwei Liu, Shuiqing Li, Adrian Baule, Hernán A. Makse

Here, we provide details on the simulation techniques used in our paper. Section I gives the computational details of a novel discrete-element method for small particles, based on an adhesive contact model (JKR theory). We denote this model as *Adhesive DEM*. The detailed simulation results, by considering different deposition velocities and particle sizes, are provided in Section II.

I. Computational method: Adhesive DEM

A newly-developed adhesive DEM approach is used in which the translational and rotational motions of all particles are evolved using the linear and angular momentum equations (see computational details in [1, 2])

$$m\frac{d\mathbf{v}}{dt}=\mathbf{F}_F+\mathbf{F}_A, \qquad I\frac{d\mathbf{\Omega}}{dt}=\mathbf{M}_F+\mathbf{M}_A, \tag{S1}$$

where $\mathbf{v}$ and $\mathbf{\Omega}$ are, respectively, velocity and rotation rate of an individual particle, m is the particle mass, and $I=(2/5)mr_p^2$ is the moment of inertia. In a vacuum system, the fluid forces and torques acting on the particle, $\mathbf{F}_F$ and $\mathbf{M}_F$, are ignored. $\mathbf{F}_A$ denotes the collision and the van der Waals adhesion forces in the equation for translational motion. Meanwhile, in the equation for rotational motion, $\mathbf{M}_A$ denotes the sum of the collision and van der Waals adhesion torques on the particle. They include,

$$\begin{aligned}\boldsymbol{F}_A&=F_n\mathbf{n}+F_s\mathbf{t}_s\\ \boldsymbol{M}_A&=r_iF_s(\mathbf{n}\times\mathbf{t}_s)+M_r(\mathbf{t}_s\times\mathbf{n})+M_t\mathbf{n}\end{aligned} \tag{S2}$$

where F_n is the normal adhesively elastic contact force, F_s is the tangential force due to the sliding friction, M_r is the rolling resistance and M_t is the twisting resistance. r_i is the particle radius. $\mathbf{n}$, $\mathbf{t}_s$

and $\mathbf{t}_r$ are the normal, tangential and rolling direction unit vectors, respectively.

Normal Elastic and Adhesive Forces

Collision and adhesion forces for fine particles are dominated by **the normal elastic and adhesive forces and the torque due to rolling resistance** that arise from the presence of the adhesive force. Forces and torques are also present to inhibit sliding and twisting motions (see [1]), but the magnitude of these two motions is small for sufficiently fine particles, e.g., micron-sized particles.

The normal force acts in the direction of the unit vector **n** which points parallel to the line connecting the centers of the two particles, denoted by *i* and *j*, such that $\mathbf{n} = (\mathbf{x}_j - \mathbf{x}_i)/|\mathbf{x}_j - \mathbf{x}_i|$. We consider two particles with radii r_i and r_j, elastic moduli E_i and E_j, and Poisson ratios σ_i and σ_j. An effective particle radius *R* and effective elastic moduli *E* and are defined by

$$\frac{1}{R} \equiv \frac{1}{r_i} + \frac{1}{r_j}, \qquad \frac{1}{E} \equiv \frac{1-\sigma_i^2}{E_i} + \frac{1-\sigma_j^2}{E_j}. \tag{S3}$$

The particle normal overlap δ_N is defined by $\delta_N = r_i + r_j - |\mathbf{x}_i - \mathbf{x}_j|$, where $\mathbf{x}_i$ and $\mathbf{x}_j$ denote the particle centroid positions. The particle normal adhesive and elastic forces are written together as $\mathbf{F}_A = F_n \mathbf{n}$, where a *Lennard-Jones* like formula for $\mathbf{F}_A$ between two particles is proposed (see more details in [2, 3]),

$$\frac{F_n}{F_C} = 4\left(\frac{a}{a_0}\right)^3 - 4\left(\frac{a}{a_0}\right)^{3/2}, \qquad \frac{\delta_N}{\delta_C} = 6^{1/3}\left[2\left(\frac{a}{a_0}\right)^2 - \frac{4}{3}\left(\frac{a}{a_0}\right)^{1/2}\right], \tag{S4}$$

which are in turn based on the JKR theory, as $a^3 = \frac{3}{4}R[F_{ne} + 3\pi Rw + \sqrt{6\pi RwF + (3\pi Rw)^2}]/E$, here $a(t)$ is the contact region radius and *w* is work of adhesion due to van der Waals interactions (namely twice the surface energy) of two contacting particles [4]. As shown in Fig. S1, the JKR model assumes that the

adhesive force is only acting inside the contact radius a, and results in a larger contact area than the classic Hertzian contact, $a > a_h$. Basically, in contrast to the DMT model (Derjaguin-Mueller-Topprov), the JKR model is appropriate for compliant, adhesive particles for which the particle's Tabor parameter is large than unity, implying the length scale of elastic deformation is large compared to the length scale of the adhesive force [2]. Then, the critical force and overlap, F_C and δ_C, and the equilibrium contact radius a_0 are given by,

$$F_C = \tfrac{3}{2}\pi w R, \qquad \delta_C = \frac{a_0^2}{2(6)^{1/3} R}, \qquad a_0 = \left(\frac{9\pi w R^2}{2E}\right)^{1/3}, \tag{S5}$$

The solution to Eq. S4 is stored prior to onset of time-stepping to build a look-up table of the normal force ratio F_n / F_C as a function of the overlap ratio δ_N / δ_C using a double interpolation algorithm. Typical values of *w* are about **10-30** mJ/m^2, from either measurements or Lifshitz theory's predictions.

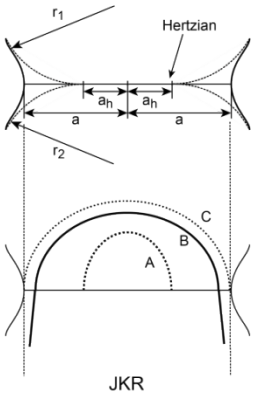

Fig. S1 Schematic diagram illustrating the stress distributions for JKR model

Effect of Adhesion on Rolling Resistance

The rolling resistance exerts a torque on the particle in the $M_r \mathbf{t}_r \times \mathbf{n}$ direction, where $\mathbf{t}_r$ is the direction of the "rolling" velocity. An expression for the rolling displacement of arbitrary-shaped

particles is derived by Bagi and Kuhn [5]. Taking the rate of this expression and specializing to spherical particles of equal size yields an equation for the "rolling velocity" $\mathbf{v}_L$ of particle *i* as

$$\mathbf{v}_L = -R(\boldsymbol{\Omega}_i - \boldsymbol{\Omega}_j) \times \mathbf{n} \ . \tag{S6}$$

An expression for the rolling resistance torque M_r is postulated in the form,

$$M_r = -k_r \boldsymbol{\xi} \cdot \mathbf{t}_r \,, \tag{S7}$$

where the direction of rolling is $\mathbf{t}_r = \mathbf{v}_L / |\mathbf{v}_L|$ and the rolling displacement is $\boldsymbol{\xi} = \int_{t_0}^{t} \mathbf{v}_L(\tau)\, d\tau$. Rolling involves an upward motion of the particle surfaces in one part of the contact region and a downward motion in the other part. The presence of an adhesive force between the two contacting surfaces thus introduces a torque resisting rolling of the particles. An expression for the rolling resistance in presence of adhesion was derived by Dominik & Tielens [3, 6], which yields the coefficient k_r as,

$$k_r = 4F_C (a / a_0)^{3/2} . \tag{S8}$$

The critical resistance occurs when the rolling displacement magnitude, $\xi = |\boldsymbol{\xi}|$, achieves a critical value, corresponding to a critical rolling angle $\theta_{crit} = \xi_{crit} / R$. For $\xi > \xi_{crit}$, the rolling displacement $\boldsymbol{\xi}$ in (S6) is replaced by $\xi_{crit}\mathbf{t}_r$. It is noted, according to the measurement by atomic force spectroscopy, θ_{crit} is around **(0.6-1.0)%** [7].

Effect of Adhesion on Sliding and Twisting Resistance

As aforementioned, both sliding and twisting are relatively rare for small adhesive particles – rolling is generally the preferred deformation mode for agglomerates of adhesive particles [2, 6]. It is therefore desirable to introduce relatively simple expressions for sliding and twisting resistance in the DEM framework. The standard sliding model for the case without adhesion is the spring-dashpot model

proposed by [8], for which the sliding force F_s is given by a linear spring-dashpot, $F_s = -k_t \delta_t \cdot \mathbf{t}_s - \eta_t \mathbf{v}_S \cdot \mathbf{t}_s$ ($\mathbf{t}_s$ is tangential direction), when $|F_s| < F_{crit}$ and by the Amonton friction expression $F_s = -F_{crit}$ when $|F_s| \geq F_{crit}$. Here, a simple model proposed by Thornton [9] and Thornton and Yin [10], agreeing reasonably well with experimental data, is introduced. In this model, the only influence of van der Waals adhesion on sliding force is to modify the critical force F_{crit} at which sliding occurs, which is given by,

$$F_{crit} = \mu_f |F_{ne} + 2F_C|, \tag{S9}$$

where F_C is the critical normal force given in (S5) and μ_f is a friction coefficient that is normally about 0.3. When particles are being pulled apart, the normal force approaches $-F_C$ at the point of separation, at which point the critical sliding force in (S8) approaches $\mu_f F_C$.

The same model with twisting resistance can be used in the presence of adhesion, with the critical force F_{crit} used to obtain $M_{t,crit} = \frac{3\pi}{16} a F_{crit}$. For twisting moments with magnitude greater than $M_{t,crit}$, the torsional resistance is given by

$$M_t = -\frac{3\pi}{16} a \mu_f |F_n + 2F_C| \, \Omega_T / |\Omega_T|. \tag{S10}$$

II. Detailed simulation results using DEM

The generation of the packing starts with the successively random free falling of 1000 uniform spheres with an initial velocity U_0 at a height H. The physical and geometrical parameters used in the DEM simulations are listed in Table S1. Firstly, a sensitivity analysis between the cases L=20r_p and L=40r_p was conducted. The parameters used and results are displayed in Table S2. As shown in Fig. S2, the difference of volume fraction of different length scales can be negligible so that L=20r_p is big enough to reproduce bulk properties. Then, as shown in Fig. S3, the particle deposition velocity (U_0), the

particle radius (r_p) and the work of adhesion (w) between the particles all significantly affect mesoscopic packing structures. The increased velocity and particle size, or decreased w results in a relatively dense packing.

Table S1. Parameters used in DEM simulations

Physical parameter	Value	Units
Particle number (N)	1000	
Particle radius (r_p)	1,5,10,50	μm
Particle density (ρ_p)	2500	kg/m^3
Work of adhesion (w)	30,20,10, 5,1	mJ/m^2
Characteristic length (L)	$20\times r_p$	μm
Particle Injection height (H)	$4\times L$	μm
Gravity acceleration (g)	9.81	m/s^2
Deposition velocity(U_0)	0.5~10	m/s

Table S2. Sensitivity analysis between cases of $L=20r_p$ and $L=40r_p$

r_p(μm)	L(μm)	U_0(m/s)	w (mJ/m^2)	N	Volume fraction	Coordination number
1	20	0.5	30	1000	0.149	2.21
1	40	0.5	30	1000	0.148	2.19

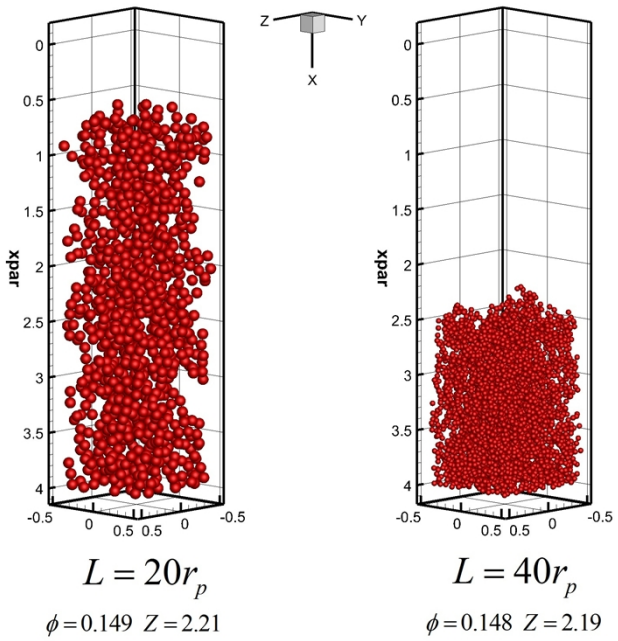

Fig. S2 The packing structures of L=20r_p and L=40r_p with other parameters being the same.

Fig. S4 further shows the volume fraction of all the simulation conditions under different sizes of particles (r_p), deposition velocities (U_0) and the work of adhesion (w). It is seen from the four sub-plots that, with increased final velocity, the volume fraction increases and then stays at a value around 0.6. However, the extent of the increment is somewhat different under variation of the particle sizes or under variation of w. For instance, for a relatively small particles (r_p=1μm), it is interesting that the very loose packing (φ=0.15) can be achieved at a low final velocity (U_0=0.5m/s) and strong adhesion (w=30mJ/m^3). When the final velocity grows to 10m/s, the volume fraction reaches 0.575 with an increment of ~0.425. However, when w goes down to 0.1mJ/m^3 (nearly non-adhesive), the volume fraction hardly changes with particle inertia U_0. On the other extreme, for much bigger particles with r_p=50μm, despite the changes of either U_0 or w, the volume fraction seems to converge to a horizontal line, which means the effects of both adhesion and particle inertia on the volume fraction is small for big particles.

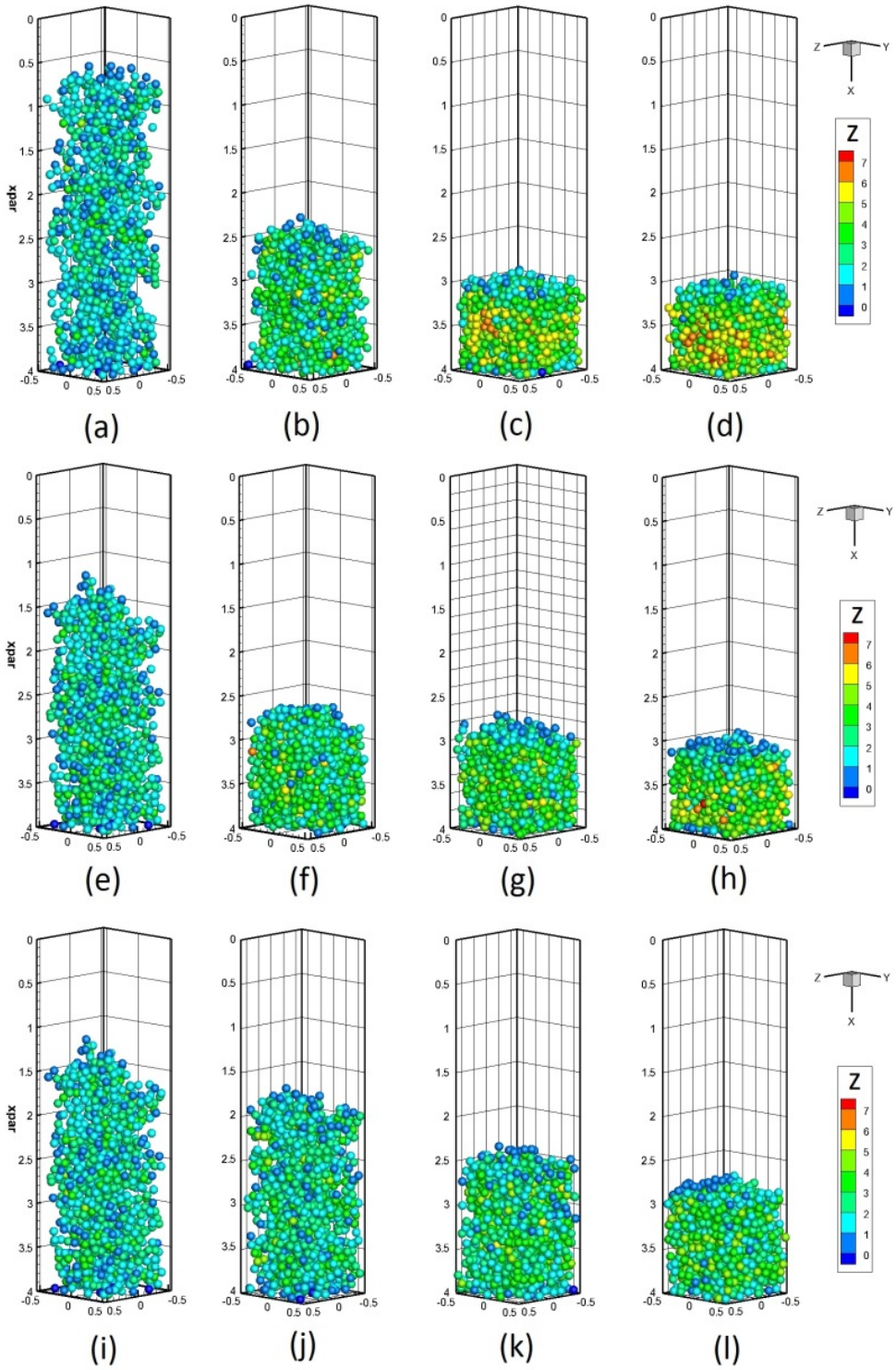

FIG. S3 Typical packing structure with different physical parameters. Different color represents different coordination number *Z*. (a)(b)(c)(d) stands for U_0=0.5, 2, 6 and10m/s, respectively with r_p=1μm and w=30mJ/m^2;
(e)(f)(g)(h) stands for r_p=1, 5, 10 and 50μm, respectively with U_0=1m/s and w=30mJ/m^2;
(i)(j)(k)(l) stands for work of adhesion w=30, 20, 10, 5mJ/m^2 respectively with r_p=1μm and U_0=1m/s.

When particles are being packed, the adhesion forces like van der Waals forces tend to attract particles and make them stick together while the particle inertia which has a quadratic correlation with particle velocity will urge them to move and impact with other particles. If adhesion is stronger than particle inertia, particles will be caught at the first impact and hardly move or roll so that a loose packing structure is easier to form. With the increase of particle sizes or velocities, particle inertia will become much stronger than the adhesion. As a consequence, more collision will take place and particles tend to be closer and form a denser packing structure.

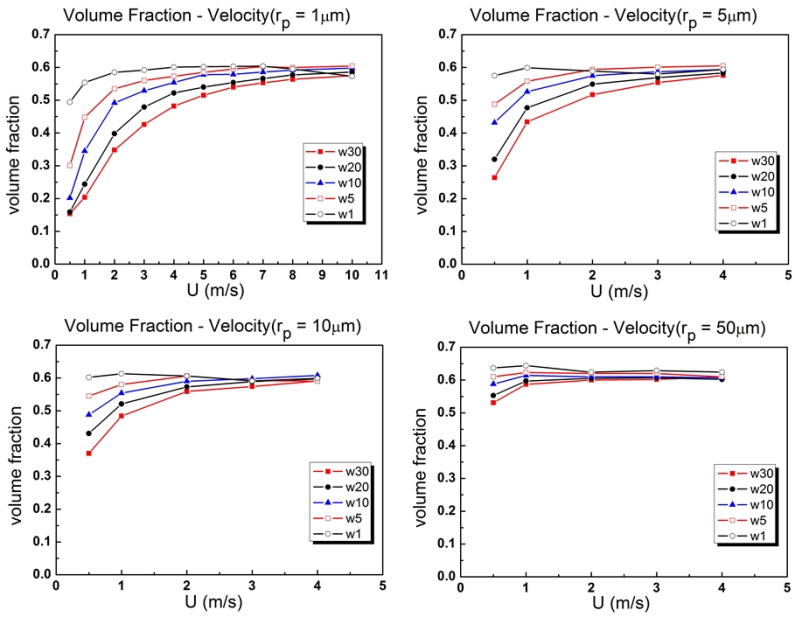

FIG. S4 Variation of volume fraction with different velocities and work of adhesion under the conditions of different sizes of particles. Left top (r_p=1μm), right top (r_p=5μm), left bottom (r_p=10μm), right bottom (r_p=50μm).

In order to interpret the balance between the interparticle adhesion and the particle inertia, we particularly employ a dimensionless adhesion parameter $Ad=w/(2\rho_p U_0^2 r_p)$, which is firstly proposed by Li and Marshall [11], as seen in details in the main text for interpreting the results of Fig. 2.

References

[1] S. Q. Li, J. S. Marshall, G. Q. Liu and Q. Yao. Prog. Energy Combust. Sci. **37**, 633-668 (2011).

[2] J. S. Marshall, S. Q. Li. Adhesive particle flow: a discrete-element approach, *Cambridge University Press*, 2014, Chapter 4, p81.

[3] C. Dominik, and A.G.G.M Tielens. Astrophys. J. **480**, 647-673 (1997).

[4] K.L. Johnson, K. Kendall, A. D. Roberts. Proc. Roy. Soc. London A **324**, 301-313(1971).
[5] K. Bagi, M.A. Kuhn, J. Apply. Mech., **71**, 493-501 (2004)
[6] C. Dominik, A.G.G.M Tielens. Philos. Mag. A, **92**, 783-803(1995).
[7] B. Sümer, and M. Sitti. J. Adhesion Sci. Technol. **22**, 481-506 (2008).
[8] P. A. Cundall, O. D. L. Strack. Geotechnique, **29**, 47-65(1979).
[9] C. Thornton, J. Phys. D-Appl. Phys. **24**, 1942-1946 (1991).
[10] C. Thornton, K. K. Yin. Powder Technol., **65**, 153-166(1991).
[11] S.Q. Li and J.S. Marshall. Journal of Aerosol Science. **38**, 1031-1046 (2007).